

## RESULTS OF RESEARCH ON BUTT JOINTS OF Q345B STEEL USING AUTOMATIC SUBMERGED ARC WELDING

Nguyen Huu Huong\*, Tong Ngoc Tuan

*Faculty of Engineering, Vietnam National University of Agriculture*

\*Correspondence to: [nhhuong@vnua.edu.vn](mailto:nhhuong@vnua.edu.vn)

Received: 02.10.2019

Accepted: 12.09.2020

### ABSTRACT

Applied research of automatic submerged arc welding for welding specific materials has real and scientific importance. Experimental implementation of the welding process of Q345B high-strength low-alloy steel with square groove butt joints presented suitable welded parameters for further study. In this study, the parameters for the welding process were obtained from investigating documents and preliminary experiments. Through the initial survey, some parameters were fixed and welding processes were carried out with input elements, and then the output parameters were evaluated to identify the essential parameters of the welding processes with a 419.5 A welding current and a 16 m/h welding speed. Based on the parameters from the experiments, calculations were performed to determine the welding processes with concrete specimens. Several essential evaluative methods were utilized to evaluate the welded quality such as the tensile test, macrostructure test, and microstructure test. In addition, initial results from the application of the automatic submerged arc welding for an equivalent sample of the machine part were presented.

Keywords: Butt joint, automatic submerged arc welding, Q345B steel.

### Một số kết quả nghiên cứu về mối hàn giáp mối của thép Q345B khi sử dụng hàn tự động dưới lớp thuốc

#### TÓM TẮT

Nghiên cứu ứng dụng công nghệ hàn tự động dưới lớp thuốc cho vật liệu cụ thể có ý nghĩa thực tiễn và khoa học. Thực hiện thí nghiệm cho quá trình hàn thép hợp kim thấp độ bền cao Q345B với mối hàn giáp mối không vát mép và có khe hở đã đưa ra được những thông số hàn phục vụ cho những nghiên cứu tiếp theo. Trong nghiên cứu này, qua nghiên cứu tài liệu và thực nghiệm sơ bộ đã xác định được một số thông số cho quá trình hàn. Qua quá trình khảo sát bước đầu, cố định một vài thông số và thực hiện quá trình hàn với thông số đầu vào và đánh giá thông số đầu ra để nhận được thông số cần thiết cho quá trình hàn với giá trị của cường độ dòng điện là 419,5 A và tốc độ hàn là 16 m/h. Dựa trên các thông số từ thí nghiệm và tính toán, thực hiện quá trình hàn với những mẫu cụ thể. Một số phương pháp cần thiết để đánh giá chất lượng của mối hàn đã được sử dụng như thử kéo, kiểm tra cấu trúc thô đại và cấu trúc tế vi. Ngoài ra, ứng dụng công nghệ hàn tự động dưới lớp thuốc cho các mẫu có hình dạng giống chi tiết máy đã thu được một số kết quả.

Từ khóa: Hàn giáp mối, hàn tự động dưới lớp thuốc, thép Q345B.

#### 1. INTRODUCTION

There are various materials that can be applied for manufacturing machine parts. These machine parts are manufactured by vastly different welding technologies such as metal inert gas (MIG) welding, metal active gas (MAG) welding, tungsten inert gas (TIG)

welding, submerged arc welding (SAW), friction stir welding (FSW), and flux core arc welding (FCAW). Automatic submerged arc welding (automatic SAW) is one of the technologies that is widely used (Karaođlu *et al.*, 2008; Ngo Le Thong, 2009). This is an ideal method for enhancing the welding quality (Karaođlu & Secgin, 2008; Ngo Le Thong, 2009). For

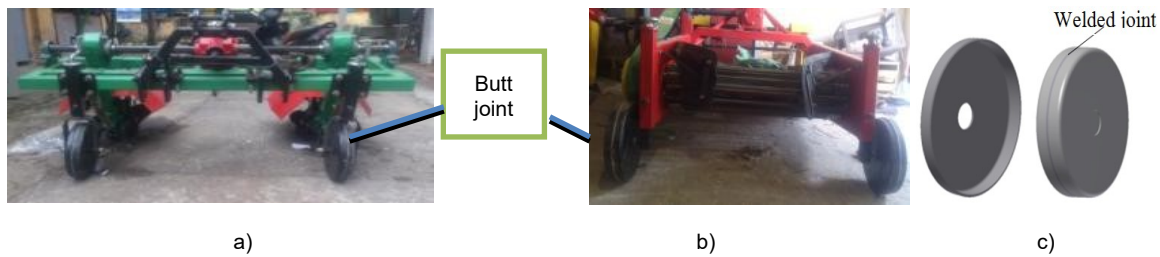
different welding types and different materials, the formulae related to the welding domain can be found in previously published documents but these must be combined with experimentation to find the reasonable values (Reddy, 2013; Vu Van Ba, 2015). Automatic submerged arc welding and suitable equipment are combined for surveying solderability when carrying out the welding processes and evaluating applicability of concrete metal materials.

High-strength low-alloy (HSLA) steel is utilized to enhance the mechanical properties and anti-corrosive ability instead of conventional carbon steel because this steel is manufactured to meet concrete demands about mechanical properties when the work is not too concerned about chemical composition. In comparison with carbon steel, HSLA steel has a much higher durability than carbon steel with the same carbon composition (Nghiem Hung, 2010). This steel has applications in manufacturing various machine parts such as brackets and bodywork, agricultural mechanical parts, and pipe and pressure vessels (ASM International, 2001; Tran Van Dich *et al.*, 2006; Ngo Le Thong, 2009; You *et al.*, 2016). Moreover, HSLA steel has good solderability so it is often applied in manufacturing welding structures (Ngo Le Thong, 2009; You *et al.*, 2016). From the various types of HSLA steel, Q345B has good mechanical properties and can be applied in different fields with specific welded structures (You *et al.*, 2016). In addition, based on published documents about materials used for manufacturing machine parts and specifically agricultural machine parts, Q345B steel was utilized in this study.

A butt joint is one of fundamental welding types that has been widely employed for manufacturing machine parts. In order to reduce preparatory time and cost before welding, the square groove butt joint was chosen for this study. The automatic submerged arc welding process has several factors that will affect the shape and dimensions of a weld (Karaođlu & Secgin, 2008; Ngo Le Thong, 2009). In this study, two main factors, namely the welding current and welding speed, were

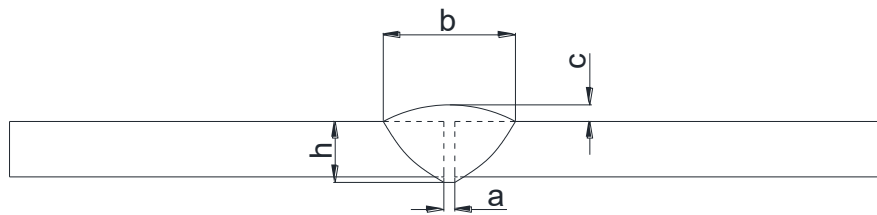
investigated with the square groove butt joint type using Q345B HSLA steel and other factors referenced from the literature (Blodgett *et al.*, 1999; Kumanan *et al.*, 2007; Lincoln Global Inc., 2014). In the laboratory, preliminary experiments were implemented to define the research zones of the welding current and welding speed. Conventional output parameters involving the penetration depth, excess cap height, and weld cap width were referenced from Karaođlu & Secgin (2008) and Reddy (2013).

In order to reduce the time and cost for preparing specimens before welding, specimens for the experiments were often simplified but still maintained good requirements for these experiments. The results from this study in coordination with further calculations can be used to weld machine parts including agricultural machine parts and others. One kind of agricultural machine part is shown in Figure 1. The wheels of this machine are shown in Figure 1c with the dimensions of 300 mm and 70 mm in diameter and width, respectively. In addition, the thickness of the materials used in the weld was 5mm. From the speed of the welding head of the welding machine we could calculate the speed of the machine part and the application process for this machine part was implemented. The wire was set at the 12 o'clock position, but we were not concerned about other positions of this wire although these positions will have an effect on the shape and dimensions of this weld. There are some differences between agriculture machine parts and other machine parts in terms of working conditions that affect the working capacity and duration of these parts. In the working process, besides the simple elements which have influence upon these parts, some other elements will affect agriculture parts such as differences in humidity, flexibility, resiliency, hardness, and abrasiveness of the ground. Based on these factors, the application of materials and technologies were always of concern when these parts were manufactured. Moreover, for general butt joints, this study will provide support for the application process and further research.



Note: a - Cultivator; b - Potato harvesting machinery; c - The structure of wheels.

**Figure 1. Parts of agricultural machines with butt joints**



Note: a - Root gap before welding; b - Weld cap width; c - Excess cap height; h - Penetration depth.

**Figure 2. Dimension parameters of the welded joint**

In order to obtain essential results, the authors utilized software including Minitab 17.3.1 and Modde 11.0.1 combined with the planning of these experiments. The experiment plan was conducted according to Nguyen Van Du & Ngo Dang Binh (2011) and Giang Thi Kim Lien (2009). These software programs provided support in building graphs and determining the effects of the welding shape parameter and welding dimensions.

## 2. MATERIALS AND METHODS

### 2.1. Research materials

Several documents (TCVN 5403:1991, An American National Standard, 2007; Ngo Le Thong, 2009; Sulaiman *et al.*, 2011) have already published suitable specimen dimensions for welding experimental processes of Q345B HSLA steel (Figure 3 and Figure 4). For Q345B HSLA steel, the chemical composition and mechanical properties were presented in the article of Tran Van Dich & Ngo Tri Phuc (2006). The reported chemical composition of the materials were  $C \leq 0.2$ ,  $Mn = 1 \div 1.6$ ,  $Si \leq 0.55$ ,  $P \leq 0.04$ ,  $S \leq 0.04$ ,  $V = 0.02 \div 0.15$ ,  $Nb = 0.015 \div 0.06$ , and  $Ti = 0.02 \div 0.2$  (mass %). The mechanical properties were

as follows: tensile strength  $\sigma_b \geq 470$  MPa, yield strength  $\sigma_y \geq 345$  MPa, and elongation  $\delta = 21\%$ . Automelt A55 welding flux (Ador welding Limited, 2015) combined with EL12 low carbon steel wire with the diameter 1.6 mm were used following the AWS F6A2/F7A0-EL12 standard. In addition, an autotractor-630-1 welding machine with armada-630 welding source was utilized in this study.

The dimension parameters of the butt joint are shown in Figure 2 and the welding model chosen had a with small gap, no padding, no bevel, and a metal thickness of 5mm.

### 2.2. Methodology

#### 2.2.1. Experimental Model

During the welding process, various factors influence the shape and dimensions of the welded joint. In order to determine these factors, the concrete parameters were found from the application of formulaic and experimental processes, and then applied in the welding machine parts. Based on all the parameters that have been researched before, the chosen factors to investigate were the welding current ( $I_h$ ) and the welding speed ( $V_h$ ). Other factors such as the welding voltage

and diameter of the wire were determined based on published documents, the welding machine, and preliminary tests. The typical factors for the shapes and dimensions of welded joints were evaluated involving penetration depth ( $h$ ), excess cap height ( $c$ ), and weld cap width ( $b$ ). From the steel plates shown in Figure 3, the build-up model for the welding process is indicated in Figure 4.

Planning of the experiment method was used to establish the regression function in order to determine the relationship between the concrete welding parameters ( $I_h, V_h$ ) and the three dimensions of welded joint ( $h, c, b$ ). The factors in the polynomial regression function were determined by analyzing the regression using Minitab software as an alternative method for variance analysis.

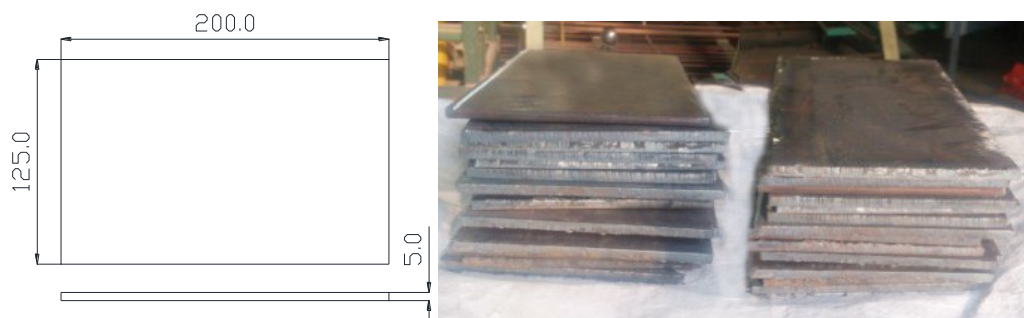


**Figure 3. Dimensions of the steel plates before welding**

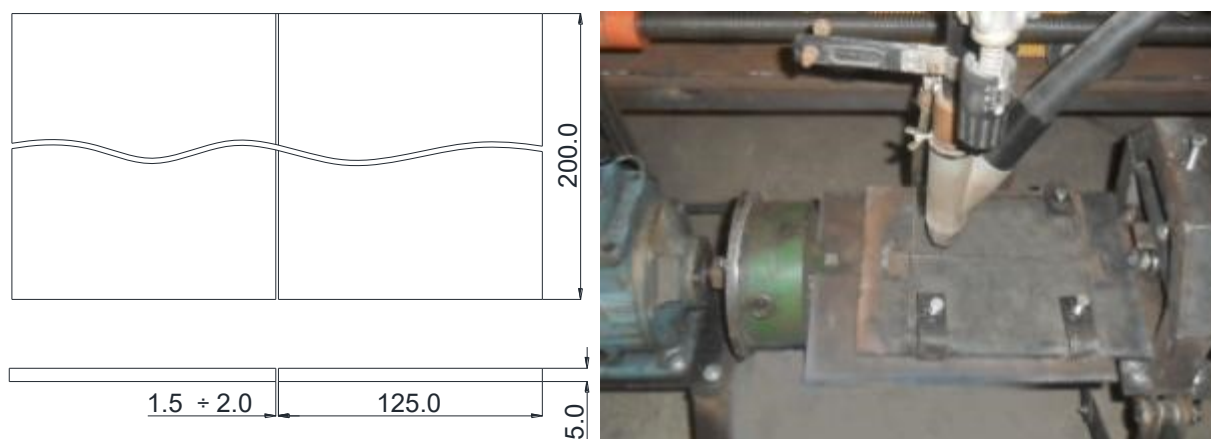


**Figure 4. Build-up model for the welding process**



**Figure 5. Experimental welding process**



Note: a - The front side of the welded joints; b - The back side of the welded joints.

**Figure 6. A selection of specimens for the visual and dimension test**

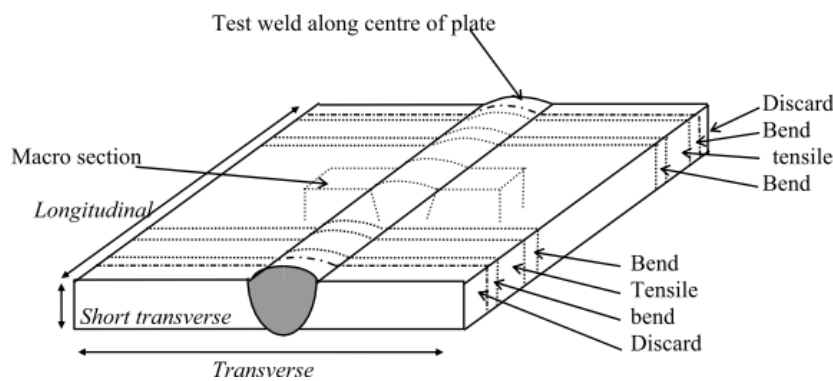


**Figure 7. Method for cutting test-pieces from the procedure approval plate**

### 2.2.2. Welding experiments

The experiments were divided into two steps: before welding and welding process, and after welding. The before welding and welding process (Figure 4 and Figure 5) involved the preparation for the build-up model, making adjustments in the calculation and selection of the welding parameters, and the implementation of the welding experiments based on specimens prepared. The after welding process (Figures 6, 8, 15, and 16) involved cleaning the specimens and preliminarily checking the welded joint, the preparation of the standard experimental pieces for the testing process, and testing the welding quality of the pieces. The method for cutting the test-pieces from the procedure approval plate is presented in Figure 7.

### 2.2.3. Evaluation of the weld quality

The standard methods for the mechanical testing of welds are indicated by the American

National Standard (2017). Standards are defined and illustrated in sections related to the bend test, tensile test, hardness test, break test, shear test, fracture toughness test, and visual test. Some of these tests are often utilized for evaluating weld quality including the visual test, dimension test, tensile test, and structural test (macrostructure test and microstructure test). The macrostructure test involves cutting the test pieces, and then grinding and etching the surface before photographing the pieces to show the macrostructure of the welded joint. The microstructure test involves the preparation of the test pieces to analyze the microstructure test zones: weld bead, heat affected zone, and unaffected base metal. The pieces for the tensile test are shown in Figure 8 based on the American National Standard (2017). The thickness (T) and width (W) of the piece were 5mm and  $38 \pm 0.25$ mm, respectively.

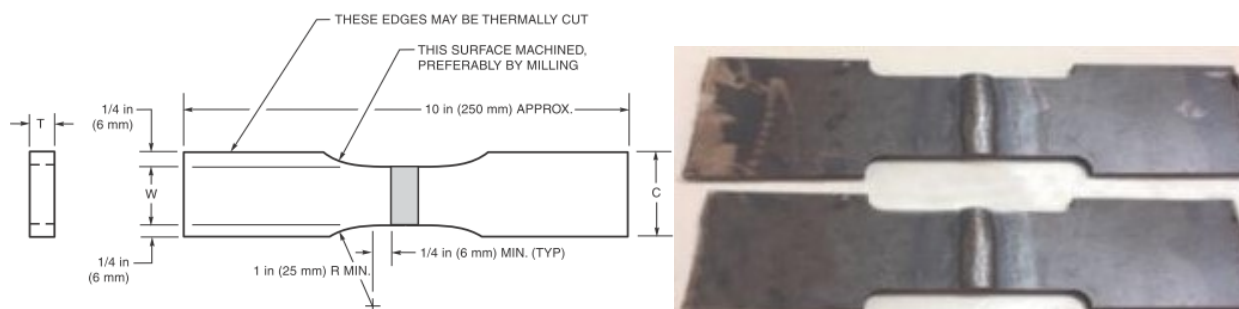


Figure 8. Transverse rectangular tension test piece

Table 1. The values and upheaval range of the input parameters

Variable	Input parameters	
	Parameter $x_1$ : $I_h$ (A)	Parameter $x_2$ : $V_h$ (m/h)
Upper level ( $Z_i = +1$ )	430	19
Basic level ( $Z_i = 0$ )	420	17
Lower level ( $Z_i = -1$ )	410	15
Upheaval range $\Delta X_i$	10	2

### 3. RESULTS AND DISCUSSION

#### 3.1. Experiments to determine the parameters of the automatic submerged arc welding process

In order to reduce the time for preparing specimens before welding, the authors chose the welding model shown in Figure 4.

Stick out of electrode: 30 mm (Blodget *et al.*, 1999)

Voltage: 25V

Welding parameters were based on the welding literature (Ngo Le Thong, 2009), guidance from the welding machine manufacturer, and preliminary experiments. In the laboratory, after the preliminary experiments, the research zones of the welding current and welding speed were determined. The research zones are shown in Table 1:

$$x_1 = 410-430A;$$

$$x_2 = 15-19 \text{ m/h.}$$

Conventional input parameters (main parameters –  $x_i$ ):

$x_1$  – Welding current,  $I_h$  (A);

$x_2$  – Welding speed,  $V_h$  (m/h).

Conventional output parameters ( $y_i$ ):

$y_1$  – Penetration depth,  $h$  (mm);

$y_2$  – Excess cap height,  $c$  (mm);

$y_3$  – Weld cap width,  $b$  (mm).

The results of the research and literature published by Yang *et al.* (1993) and Kumanan *et al.* (2007), and based on the results of the preliminary experiments indicated that the welding dimensions (penetration depth, excess cap height, and weld cap width) depended on the factors of the welding conditions (welding current and welding speed):

Equivalent function:

$$y_i = a_0 + a_1x_1 + a_2x_2 + a_{12}x_1x_2 \quad (3.1)$$

Based on the expected model with first-order linearity, the authors set the experimental points

$N \geq 2k = 22 = 4$ , with  $k$  being a survey variable. Table 2 shows the experimental matrix with both the real variables and code variables. In order to enhance accuracy, each experiment was carried out three times and the average values were calculated (Table 3). In addition, Table 4 illustrates the results of three experiments which were implemented at center.

**Table 2. Experimental matrix**

No.	Real variable		Code variable	
	$I_h$ (A) $x_1$	$V_h$ (m/h) $x_2$	$Z_1$	$Z_2$
1	410	15	-1	-1
2	430	15	+1	-1
3	410	19	-1	+1
4	430	19	+1	+1
5	420	17	0	0
6	420	17	0	0
7	420	17	0	0

**Table 3. Experimental results**

No.	Welding parameters		Output parameters (mm)			Note
	$I_h$ (A)	$V_h$ (m/h)	$h$	$c$	$b$	
1	410	15	4.3	1.9	13.5	
2	430	15	5.7	3.2	14.3	
3	410	19	3.5	2.4	11.4	
4	430	19	5.1	3.6	12.0	

**Table 4. Experimental results at center**

No.	Welding parameters		Output parameters (mm)			Note
	$I_h$ (A)	$V_h$ (m/h)	$h$	$c$	$b$	
1	420	17	3.9	2.7	12.6	
2	420	17	4.6	3.3	11.9	
3	420	17	4.2	2.8	12.8	
(Average value at m times of measurement)			4.23	2.93	12.43	

**Table 5. Regression factors from the experimental process**

	$a_0$	$a_1$	$a_2$	$a_{12}$
$h(y_1)$	4.65	0.75	-0.35	0.05
$c(y_2)$	2.775	0.625	0.225	-0.025
$b(y_3)$	12.8	0.35	-1.1	-0.05

Utilizing Minitab 17.3.1 software, we determined the factors of the experimental regression function with the general equivalent function (3.1). Table 5 shows the values of the regression factors from the experiments with penetration depth ( $h$ ), excess cap height ( $c$ ), and weld cap width ( $b$ ).

From the results above we obtained the experimental regression equations:

$$y_1 (h) = 4.65 + 0.75x_1 - 0.35x_2 + 0.05x_1x_2 \tag{3.2}$$

$$y_2 (c) = 2.775 + 0.625x_1 + 0.225x_2 - 0.025x_1x_2 \tag{3.3}$$

$$y_3 (b) = 12.8 + 0.35x_1 - 1.1x_2 - 0.05x_1x_2 \tag{3.4}$$

Based on the results from the Minitab 17.3.1 software, the experimental regression

equations when excluding all values that have p much larger than significance level  $\alpha$  (0.05) are as follows:

$$y_1 = 4.65 + 0.75x_1 - 0.35x_2 \tag{3.5}$$

$$y_2 = 2.775 + 0.625x_1 + 0.225x_2 \tag{3.6}$$

$$y_3 = 12.8 + 0.35x_1 - 1.1x_2 \tag{3.7}$$

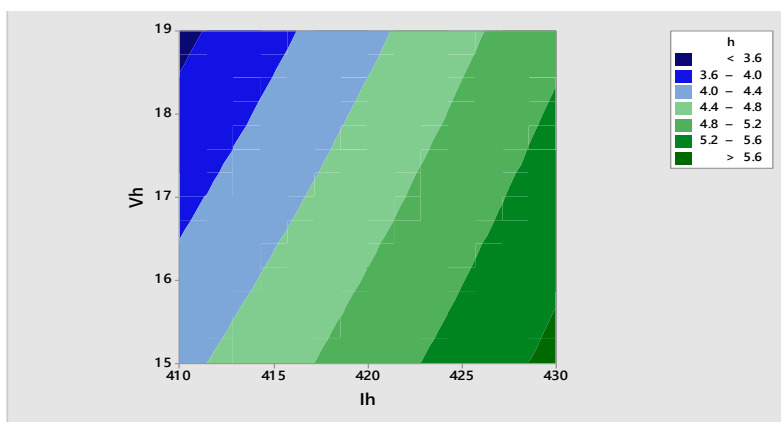


Figure 9. Simultaneous affection of  $I_h$  and  $V_h$  to penetration depth (h)

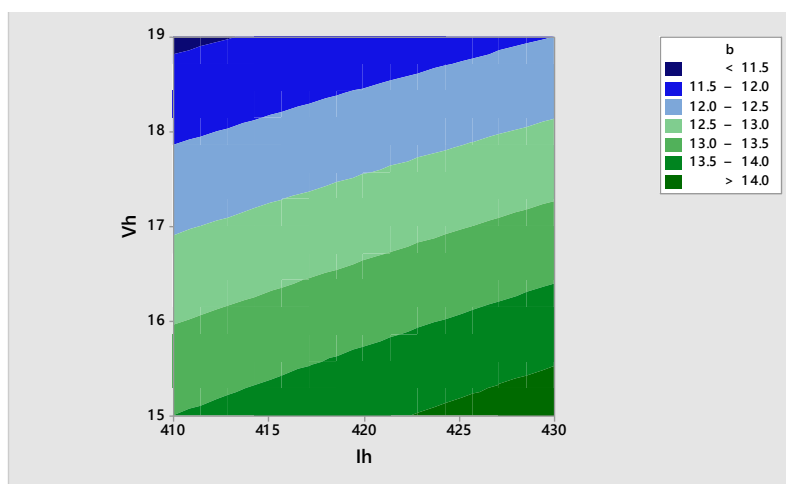


Figure 10. Simultaneous affection of  $I_h$  and  $V_h$  to welding cap width (b)

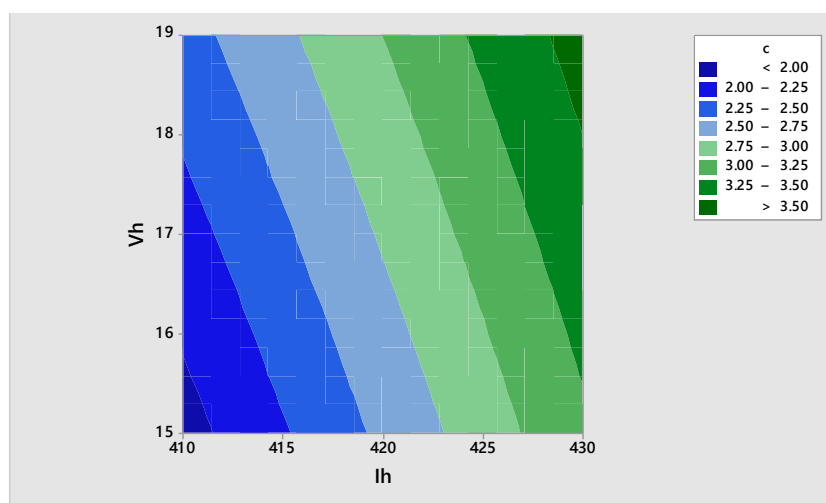


Figure 11. Simultaneous affection of  $I_h$  and  $V_h$  to excess cap height (c)

Figure 9, Figure 10, and Figure 11, and the experimental regression equations (3.5, 3.6, and 3.7) show the results related to the welding parameters and welding dimensions. The welding current ( $I_h$ ) and welding voltage ( $V_h$ ) factors simultaneously affected penetration depth (h) and welding cap width (b) in the opposite direction (+0.75 and -0.35, respectively for h, and + 0.35 and - 1.1, respectively for b). This means that increasing  $I_h$  and decreasing  $V_h$  resulted in increases in h and b, and conversely, decreasing  $I_h$  and increasing  $V_h$  resulted in decreases in h and b. On the other hand, the factors  $I_h$  and  $V_h$  simultaneously influenced welding cap height (c) in the same direction (+0.625 and +0.225, respectively) with an increase of  $I_h$  and  $V_h$  inducing a decrease of c, and conversely, a decrease of  $I_h$  and  $V_h$  inducing a decrease of c.

The pieces cut from the experimental specimens for testing the macrostructure were used to determine the desired dimensions of the welded joint, and the weld bead was evaluated for ensuring that there were no hot toe cracks or large deformations of the welded joint. The penetration coefficient of the weld (inside shape coefficient of the weld) is  $\phi_n = b/h$  with a value from 0.8 to 4, and an optimal value of  $\phi_n$  from 1.3 to 2 (Thong, 2009). In addition, in order to ensure an equally metallic transition from the weld into the base metal, without a stress concentration phenomenon, a decrease of the weld deformation, or an increase of the strength of the welded joint under dynamic load, the value of the shape coefficient of the welded joint (outside shape coefficient of the welded joint) is often  $\phi_n = b/c = 7-10$  (Thong, 2009). Based on the above information and the experimental welding process, the correlation of the penetration coefficient and the shape coefficient of the welded joint, the experimental pieces and

the experiences through the welding process were evaluated to determine the desired dimensions of the welded joint. The value of the penetration depth, the welding cap, and the excess cap height were 4.5-5.5mm, 12.5-13.5mm, and 2.0-3.0mm, respectively, as shown in Table 6.

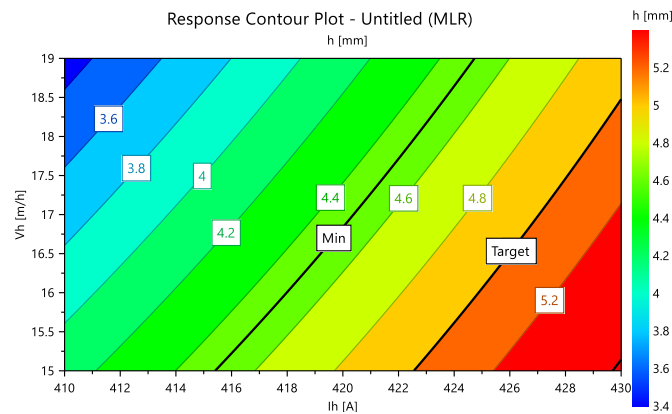
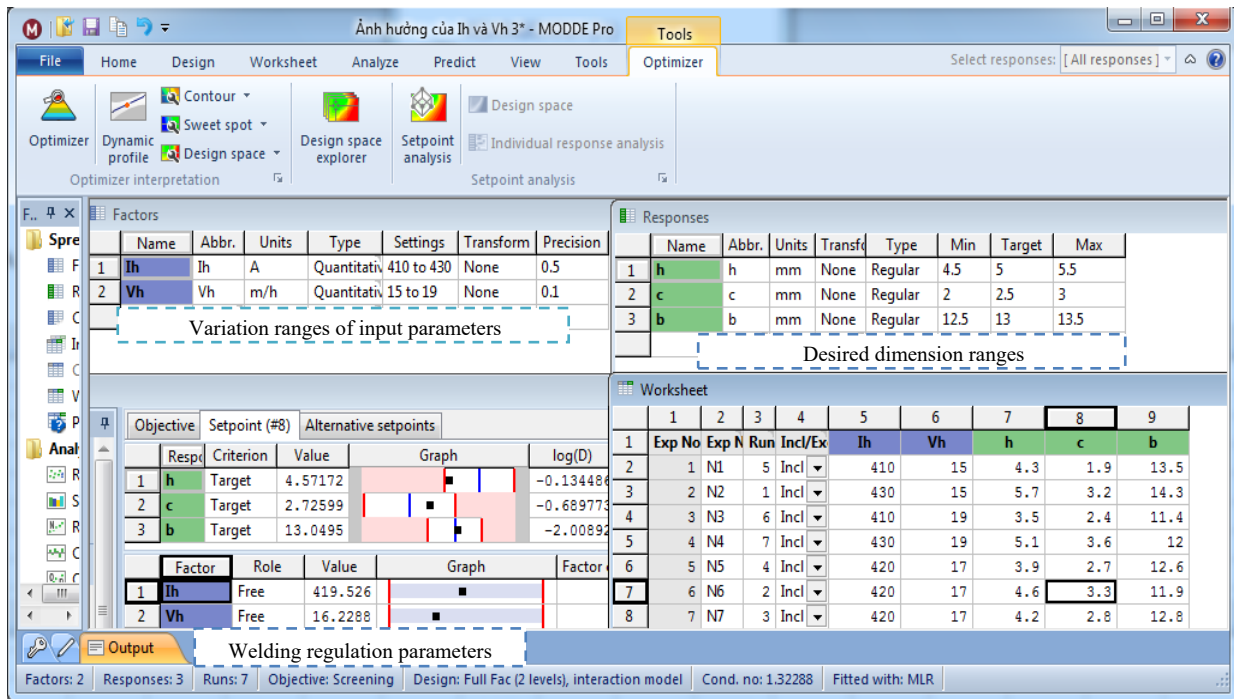
Using the “Optimizer” tool of the Modde 11.0.1 software determined the welding regulation parameters suitable for the desired dimensions (MKS Umetrics, 2014; Vu Van Ba, 2015). The input parameters with the verified research zones and the desired dimensional parameters were entered in this software program. Then, this software figured out the welding regulation parameters of  $I_h$  and  $V_h$ . According to the variation ranges of the input parameters of  $I_h$  and  $V_h$  indicated in Table 1, the desired dimension ranges of h, c, and b shown in Table 6, and the number of experiments with the results shown in Table 3 and Table 4, the welding regulation parameters of  $I_h$  and  $V_h$  were determined. The values, including the variation ranges of the input parameters, the welding regulation parameters, and the desired dimension ranges, are shown in Table 7. From Table 7, the values containing  $I_h$  and  $V_h$  obtained from Modde 11.0.1 software were about 419.5 A and 16.2 m/h, respectively. In addition, with the values of  $I_h$  and  $V_h$  determined, the values of h, c, and b were also indicated as approximately 4.6 mm, 2.7 mm, and 13.0 mm, respectively.

Figure 12, Figure 13, and Figure 14 show the minimum values, maximum values, and results at the center (target) as the  $I_h$  ( $x_1$ ) and  $V_h$  ( $x_2$ ) values changed in the research zone. In addition, the desired dimension ranges from Table 6 in proportion to the minimum, maximum, and target values are shown in Figure 12, Figure 13, and Figure 14.

**Table 6. Desired dimension ranges of the welded joint**

Penetration depth (h)	Welding cap width (b)	Excess cap height (c)
4.5 ÷ 5.5	12.5 ÷ 13.5	2 ÷ 3

**Table 7. Welding parameters based on the desired dimension ranges of the welded joint**



**Figure 12. Simultaneous affection of  $V_h$  and  $I_h$  to penetration depth ( $h$ ) with desired dimensions**

### 3.2. Evaluating the welding quality

#### 3.2.1. Tensile test

One of the methods for evaluating the welding quality is the tensile test. The pieces were cut with the standard dimensions as shown in Figure 8.

Figure 15 shows the pieces after the tensile test. These pieces were broken at the position between the weld bead and the heat-affected zone. This matter could be explained because

the arc temperature was too high for the participation of the base metal in these welds and also the diffusion of the weld bead into the base metal increased. These problems above induced a reduction of the tensile strength. On the other hand, because the shape coefficient was smaller than seven, the transition process of the weld bead into the base metal was not equal and thus, the stress concentrations increased (Ngo Le Thong, 2009). From the tensile strength test, the average fracture load

of the welds was approximately 83.0 kN in these experiments. If the welded zone was assumed from the inserted zone of the experimental pieces, the weld strength was about 425 N/mm<sup>2</sup>. The strength value of the weld per welded zone was slightly lower than the value of the base metal.

**3.2.2. Macrostructure and microstructure tests**

Macrostructure Test: After the welding process, the pieces for the macrostructure test

were made by a simple cutting machine. These pieces were sharpened flat and shined using different sandpapers. After that, the pieces were etched with an etching solution made up of 4 percent nitric acid in alcohol, and the pieces were washed and desiccated. Based on the preparation process above, the zones of the welded joint including the weld bead, heat affected zone, and unaffected base metal were distinguished. The specimens were welded with the parameters that were calculated from experiments, and toe cracks and slag did not appear on these welds.

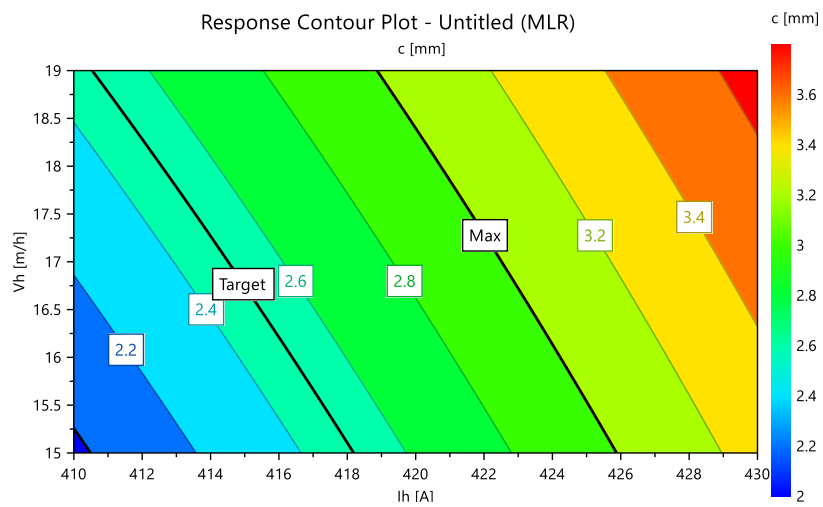


**Figure 13. Simultaneous affection of  $V_h$  and  $I_h$  to excess cap height (c) with desired dimensions**

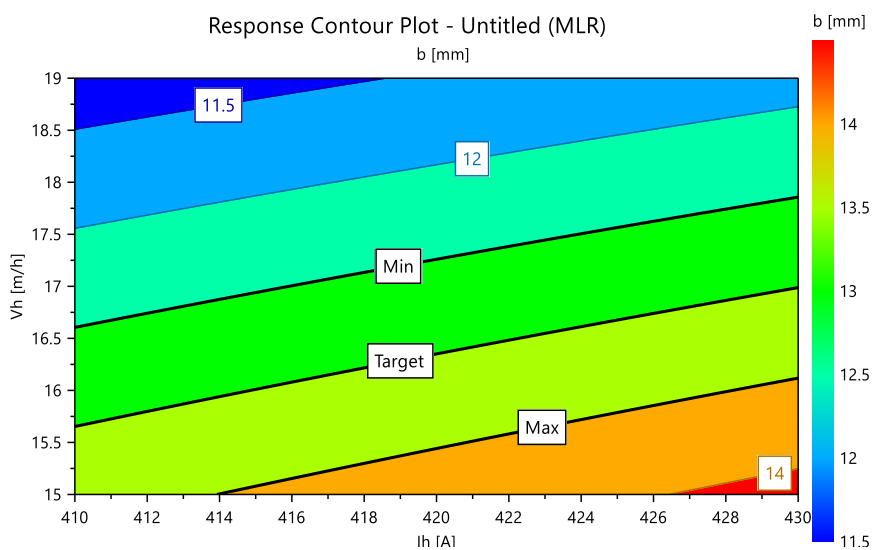


**Figure 14. Simultaneous affection of  $V_h$  and  $I_h$  to welding cap width (b) with desired dimensions**



Figure 15. Pieces after the tensile test

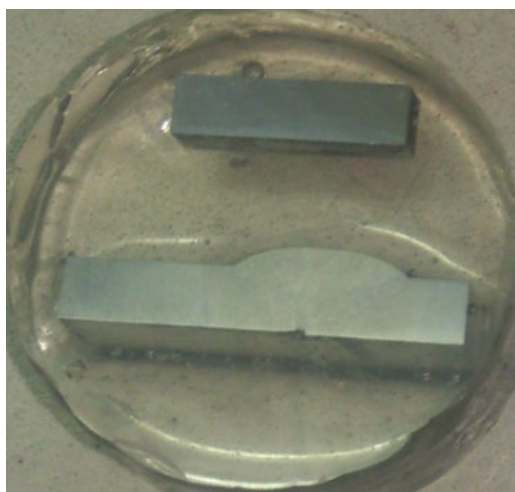


Figure 16. Pieces for the microstructure test

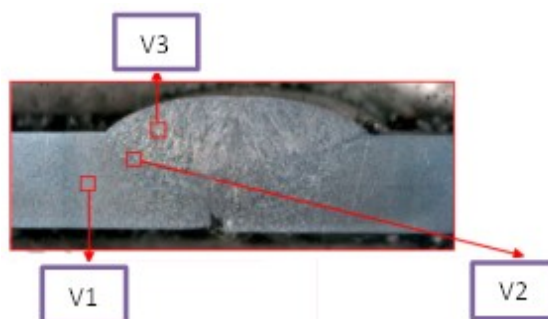


Figure 17. Microstructure survey zones of a welded joint

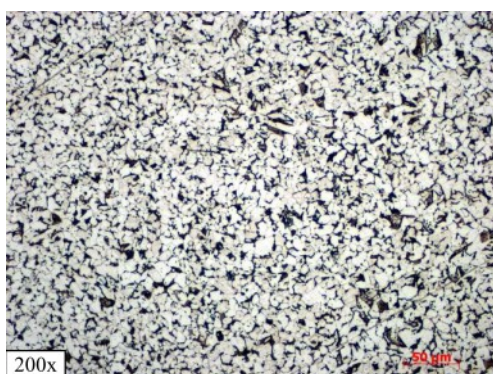
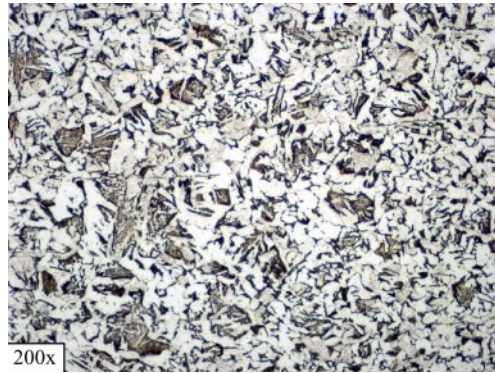
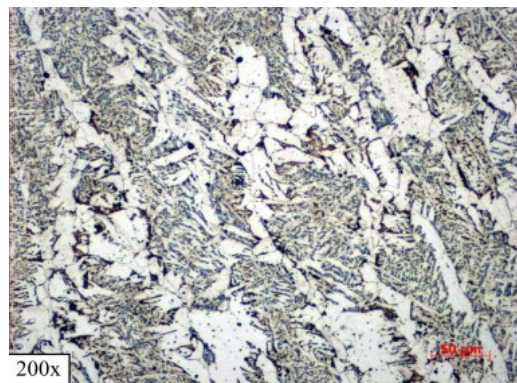


Figure 18. Microstructure of the unaffected base metal zone (V1)



**Figure 19. Microstructure of the heat-affected zone (V2)**



**Figure 20. Microstructure of the weld bead zone (V3)**

Microstructure test: The pieces for the microstructure test were cut using a CNC wire cutting machine so that no heat-affected phenomena would appear on the surface of the pieces. The test pieces and testing process were implemented in laboratories.

Figure 17 shows the three microstructure survey zones, namely the unaffected base metal zone (V1), heat-affected zone (V2), and weld bead zone (V3). The microstructure of the three zones contained ferrite and pearlite in the unaffected base metal, ferrite and bainite in the heat-affected zone, and grain boundary ferrite and bainite in the weld bead as shown in Figure 18, Figure 19, and Figure 20, respectively. The microstructure of the unaffected base metal (V1) was ferrite and pearlite with the metal grains disposed relatively equally, and having no steady guide. This was a result of the heat treatment process. The microstructure of the heat-affected zone (V2) was ferrite and bainite. At this zone, the grain dimension increased a

great deal when compared with the grain dimension of the unaffected base metal zone. From the microstructure, we could discover that the heat affected area in this zone and the metal contexture was of the overheated style. The microstructure of the weld bead (V3) was grain boundary ferrite and bainite. The ferrite contexture of the weld bead was a light grain with a multidirectional shape and a bainite contexture was established from the crystallizing process. In the microstructure test process, the ferrite contexture thrust through the bainite contexture and occurred beside this contexture. The structure of the bainite had different direct lines consisting of bright-lines and dark-lines, so the structure of the bainite was a striated type. Moreover, the metallographic examination indicated that the microstructure of the steel appeared to be a bainite contexture, and the slag and porosity phenomena did not happened. This could be explained because of the slow welding speed.

### 3.3. Application for welding a concrete sample type

Figure 18 shows the model of the welding process for agricultural machine parts.

Figure 19 shows the welding process with the parameters obtained from the experiments above, and a sample received after this process. In this welding process, the wire was set at the 12 o'clock position. Based on an initial evaluation using a visual test, the welded joint was relatively stable, not undercut, and there were no toe cracks.

### 4. CONCLUSIONS

Based on theoretical research, equipment, automatic submerged arc welding, real materials, and welding experimental processes, specific welding parameters to weld Q345B with a concrete depth were determined. Specific methods for evaluating quality including the macrostructure test, microstructure test, and tensile test of square groove butt joints were chosen. The results of this study can provide essential information for further investigation about this material and its application in manufacturing machine parts.

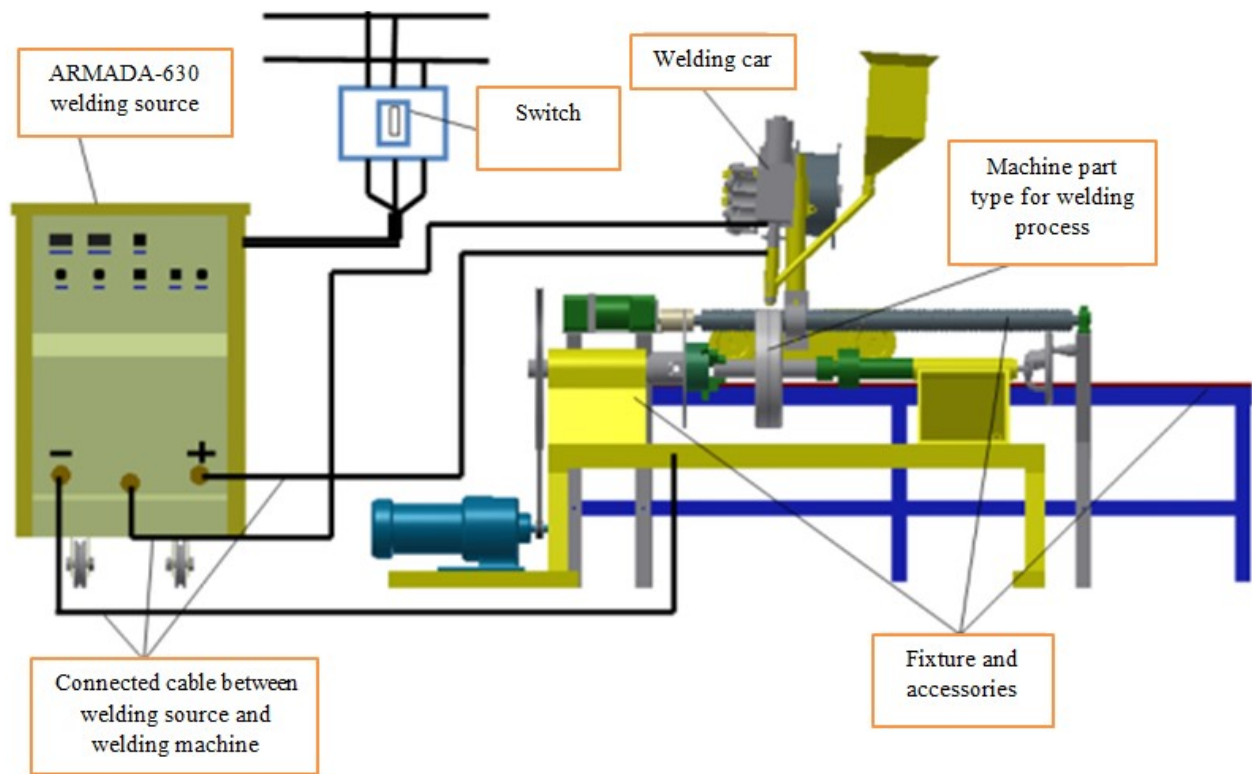


Figure 18. Model of the welding process for agricultural machine parts



Figure 19. Welding process with sample based on fixture manufactured

## REFERENCES

- An American National Standard (2007). Standard methods for mechanical testing of welds. Copyright American Welding Society.
- Ador welding Limited (2015). Automelt A55 (Automelt Gr II). Maharashtra, India. Retrieved from [http://www.adorwelding.com/index.php?option=com\\_content&view=article&id=68&Itemid=208&cat1=Welding%20Consumables#](http://www.adorwelding.com/index.php?option=com_content&view=article&id=68&Itemid=208&cat1=Welding%20Consumables#) on March 14, 2016.
- ASM International (2001). High-strength low-alloy steels. Materials Park, Ohio, USA.
- Blodgett O. W., Funderburk R. S., Miller D. K. & Quintana M. (1999). Fabricators' and Erectors' guide to welded steel construction. The James F. Lincoln Arc welding Foundation, Florida, USA.
- Giang Thi Kim Lien (2009). Lecture of planning of experiments. The University of Danang, Danang (in Vietnamese).
- ISO 4136:2012. Destructive tests on welds in metallic materials – Transverse tensile test.
- Karaođlu S. & Secgin A. (2008). Sensitivity analysis of submerged arc welding process parameters. *Journal of Materials Processing Technology*. 202(1-3): 500-507.
- Kumanan S., Raja Dhas J.E. & Gowthaman K. (2007). Determination of submerged arc welding process parameters using Taguchi method and regression analysis. *Indian journal of Engineering and Materials Sciences*. 14: 177-183.
- Lincoln Global Inc. (2014). Hardfacing product and procedure selection. 22801 St. Clair Avenue, Cleveland, U.S.A.
- MKS Umetrics (2014). User guide to Modde. 1992-2014 MKS Umetrics AB, Sweden.
- Nguyen Van Du & Ngo Dang Binh (2011). Planning of experiments in Engineering textbook. Publishing House for Science and Technology, Hanoi (in Vietnamese).
- Nghiem Hung (2010). Fundamental mechanics materials textbook. Publishing House for Science and Technology, Hanoi (in Vietnamese).
- Ngo Le Thong (2009). Fusion electric welding technology textbook, volume 1. Publishing House for Science and Technology, Hanoi (in Vietnamese).
- Reddy K.S. (2013). Optimization & prediction of welding parameters and bead geometry in submerged arc welding. *International Journal of Applied Engineering Research and Development*. 3: 1-6.
- Sulaiman M.S., Manurung Y.H., Haruman E., Abdun Rahim M.R., Redza M.R., Ak. Lidam R.N., Abas S.K., Tham G. & Chau C.J. (2011). Simulation and experimental study on distortion of butt and T-joints using weld planner. *Journal of mechanical science and technology*. 25(10): 2641-2646.
- TCVN 5403:1991. Weld-method of fractional test (in Vietnamese).
- Tran Van Dich & Ngo Tri Phuc (2006). World steel manual textbook. Publishing House for Science and Technology, Hanoi (in Vietnamese).
- Vu Van Ba (2015). Research on the one side butt weld technology applied in assembly of the ship's hull block. PhD thesis, Hanoi University of Science and Technology (in Vietnamese).
- Yang L., Bibby M. & Chandel R. (1993). Linear regression equations for modelling the submerged arc welding process. *J. of Materials process technology*. 39: 33-42.
- You X., Liu Y.J., Khan M.K. & Wang Q.Y. (2016). Low cycle fatigue behavior and life prediction of Q345B steel and its welded joint. *Materials Research Innovations*. 19: 1299-1303.